Journal of Thermal Engineering, Vol. 6, No. 1, pp. 50-57, January 2020
Yildiz Technical University Press, Istanbul, Turkey

COMPARATIVE MAXIMUM POWER DENSITY ANALYSIS OF A SUPERCRITICAL CO_2 BRAYTON POWER CYCLE

A. Sinan Karakurt[1,*], Veysi Bashan[1], Yasin Ust[1]

ABSTRACT

The supercritical CO_2 (s-CO_2) power cycle has been taking into account as one of the most effective alternatives for energy conversion because of its higher efficiency and smaller compressor and turbine sizes for many years. A plenty number of parametric and experimental studies for the different type of s-CO_2 cycles have been accomplished in the literature. In this paper, a performance analysis based on a power density criterion has been carried out for a simple s-CO_2 Brayton power cycle. The parameters which are obtained from analyzes were compared with those of a power performance criterion that is shown that design parameters at maximum power density give a chance to smaller cycle components and more efficient s-CO_2 Brayton power cycle. Due to loses in the cycle, the power and thermal efficiency will reduce by a certain amount, however, the maximum power density conditions will still give a better performance than at the maximum power output conditions. The analysis exemplified in this paper may provide a reference for the finding of optimal operating conditions and the design parameters for real s-CO_2 Brayton power cycles.

Keywords: *Power Density, Supercritical CO_2 Cycle, Brayton Cycle, Thermodynamics*

INTRODUCTION

The Brayton cycle based on supercritical carbon dioxide (s-CO_2) as the working fluid is an innovative concept for converting thermal energy to electrical energy. There is a sufficiently long history of s-CO_2 cycles. When open sources literature were examined the first application noticed, seems to be the patched half-condensation CO_2-Brayton cycle which belongs to the Sulzer brothers [1]. Although studies on this topic have not been continued adequately after this date, the main works that draw attention to these cycles have been studies of supercritical thermodynamic power cycles made by Feher in 1962 [2] and in 1968 [3]. It is widely known that, supercritical phase is a phase when an element properties between liquid and gas at critical temperature (T_c) and critical pressure (P_c). Fluids in the supercritical phase have liquid-like densities and act as a liquid solvent. As it is known, CO_2 has high heat capacity with low viscosity and mass transfer property. Surface tension coefficients, viscosities are low and therefore the pumping energy is low. CO_2 gas is not corrosive in the dry environment. It is not flammable, explosive or toxic and also is not harmful to the environment. The critical temperature for CO_2 is 304.3 K and the critical pressure is 7.38 MPa [4]. Benefits that will be reveal from successful research and development of the s-CO2 power conversion cycle will include, several heat sources including fossil fuel, nuclear and renewables such as nuclear energy, solar energy, geothermal energy, waste heat recovery and coal power plants [5–10]. Also, this technology will lead to lower capital costs and reduced water usage and most importantly lower emissions. Briefly, system is comprehensively feasible and worthy. The technology readiness can be divided into three parts. Mature components, less-mature components and system integration. Mature components contain electrical generation subsystems, control units and instrumentation. Less mature components contain turbine, heater etc. Lastly, system integration is needed to optimize the operating and design parameters and also systems start-up, shut-down, transient and part load operations of the system.

Numerous studies have been carried out in different fields on s-CO_2 power cycles. These studies consist of; thermodynamic cycle models and s-CO_2 cycles on commercial or research-based tests [11–16]. In addition, studies on the real-time response of s-CO_2 power cycles and the development of cycle control strategies [17–19], furthermore, research on turbo machines specially designed for s-CO_2 flow and on air bearings and seals with turbo machine subcomponents [20–23], the work consists of studies on high speed electric motor technologies which is essential component for the s-CO_2 cycles to be compact [24–28] and material investigations on the interaction of different materials with s-CO_2 fluid under high temperature and pressure [29–32]. Apart from these studies, there is no doubt that one of the parameters that must be taken into consideration is the maximum power

This paper was recommended for publication in revised form by Regional Editor Tolga Taner
[1]Department of Naval Architecture and Marine Engineering, Yildiz Technical University, 34349, Istanbul, Turkey
**E-mail address: asinan@yildiz.edu.tr*
Orcid ids: 0000-0002-6205-9089 , 0000-0002-1070-1754 , 0000-0002-4023-3226
Manuscript Received 7 February 2018, Accepted 23 February 2018

density (*MPD*) when performing cycle optimization. There are many studies in the literature that have been done with *MPD* in cycle analysis [33–36]. Şahin et al. [37] defined the power density as the ratio of power to the specific volume in the cycle and obliquely added the effects of engine sizes to the analysis which leads to smaller and more efficient engines. Likewise, Gonca et al. [38] studied comprehensive analyses and comparisons for irreversible cycle engines and they examined effects of design parameters on *MPD*. Likewise, Chen et al. [39] investigated advantages and disadvantages of *MPD* design analysis to observe effects of some design parameters. And they concluded that *MPD* leads to a better efficiency at cycle analysis. Apart from prior studies, in this study, comprehensive comparison parameters which are obtained from analyzes were compared with those of a power performance criterion. It is shown that design parameters at maximum power density give a chance to smaller cycle components and more efficient s-CO_2 Brayton power cycle.

THERMODYNAMIC MODEL

Schematic and T-s diagrams of closed loop ideal Brayton cycle are shown in figure 1. An isentropic compression occurs between 1 and 2 in a compressor, constant-pressure heat addition between 2 and 3 then isentropic expansion occurs between 3 and 4 in a turbine then it follows with a constant pressure heat rejection between 4 and 1 which finish the whole cycle.

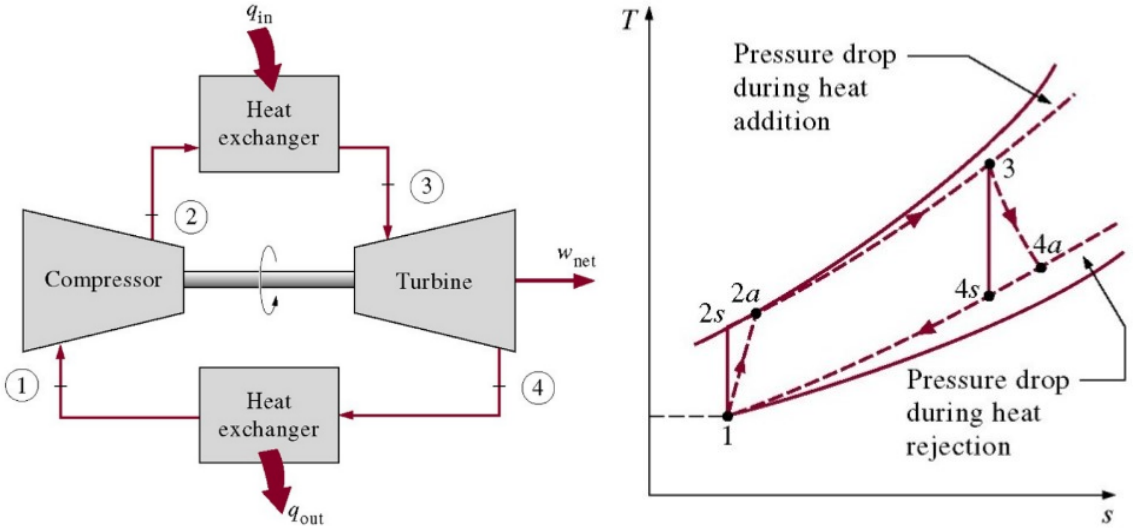

Figure 1. Schematic and T-s diagrams of a Brayton power cycle [4]

The energy balance for a steady-state flow process of ideal Brayton cycle can be expressed as below:

$$\left(q_{23}-q_{41}\right)+\left(w_{in}-w_{out}\right)=\left(h_{out}-h_{in}\right) \tag{1}$$

As known, heat transfer occurs to the working fluid and likewise from the working fluid are, respectively,

$$q_{23}=\left(h_3-h_2\right)=c_p\left(T_3-T_2\right) \tag{2a}$$

and

$$q_{41}=\left(h_4-h_1\right)=c_p\left(T_4-T_1\right) \tag{2b}$$

With regards to the cold air standard assumptions the thermal efficiency of the ideal Brayton cycle becomes:

$$\eta_{th} = \frac{w_{net}}{q_{23}} = 1 - \frac{q_{41}}{q_{23}} = 1 - \frac{c_p\left(T_4 - T_1\right)}{c_p\left(T_3 - T_2\right)} = 1 - \frac{T_1\left(\frac{T_4}{T_1} - 1\right)}{T_2\left(\frac{T_3}{T_2} - 1\right)} \tag{3}$$

While processes of 1-2 and 3-4 are isentropic, $P_2=P_3$ and $P_4=P_1$. Thus,

$$\frac{T_2}{T_1} = \left(\frac{P_2}{P_1}\right)^{\left(\frac{k-1}{k}\right)} = \left(\frac{P_3}{P_4}\right)^{\left(\frac{k-1}{k}\right)} = \frac{T_3}{T_4} \tag{4}$$

Substituting equation (4) into the equation (3) and then re-arranging becomes:

$$\eta_{th} = 1 - \frac{1}{r_p^{\left(\frac{k-1}{k}\right)}} \tag{5}$$

where r_p is the pressure ratio and k is the specific heat ratio. Apart from above equations, *MPD* can be expressed as below and it can be used as work density instead of power density:

$$MPD = \frac{w_{net}}{v_{max}} \tag{6}$$

RESULTS AND DISCUSSION

In the calculations, the constants are considered as, ambient temperature and pressure are 298 K and 100 kPa, respectively. Compressor and turbine isentropic efficiencies are 0.90 and pressure drop at heat exchangers (ΔP) is 0.03 bar. Generally, increasing the pressure ratio of a Brayton cycle is the most effective way that increases the overall thermal efficiency which cause the cycle to approach the Carnot cycle. When Figure 2 is examined, it can be seen that *MPD* increases to a certain value with increasing r_p and then begins to decrease when approximately r_p is 9.286. Likewise, η_{th} and r_{bw} of the s-CO2 cycle is also seen to increase with increasing r_p When considering α is 2.5 and constant as figure 2, the cycle thermal efficiency is 24.83%, 25.28% and 25.47%, respectively, by increasing r_p from 8.673 to 9.898 and 11.

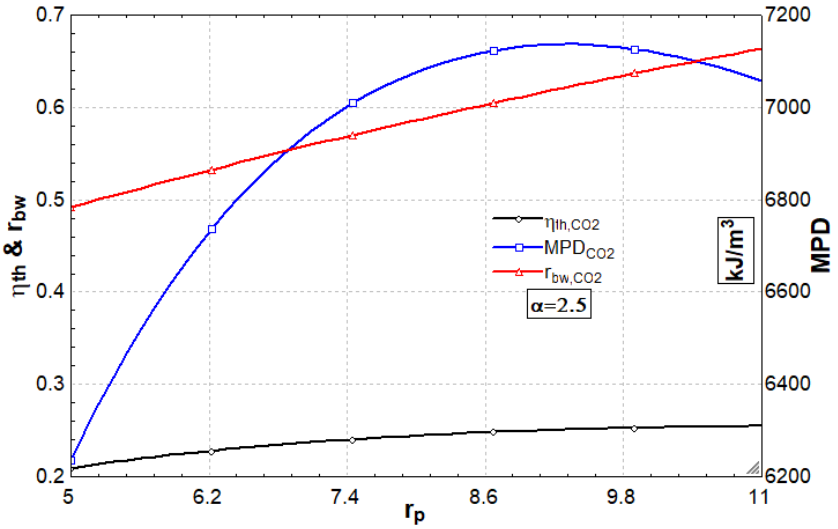

Figure 2. Variation of α on η_{th}, r_{bw} and *MPD* with respect to r_p

The turbine inlet temperature (TIT) is known to be limited by the thermal resistance limits of the turbine materials can withstand. Therefore, the temperature ratio must be within a certain range. When the temperature ratio is optimized, the efficiency of the cycle must also be considered. Figure 3 shows that when the pressure ratio is 7, there is an increase in *MPD* and thermal efficiency with increasing the temperature ratio from 2.5 to 3.5. In contrast to this situation, the rate of back work ratio decrease with the increase in the temperature ratio. While r_p is 7 and constant, increasing α from 2.908 to 3.5 value, *MPD* increases 14.89 %.

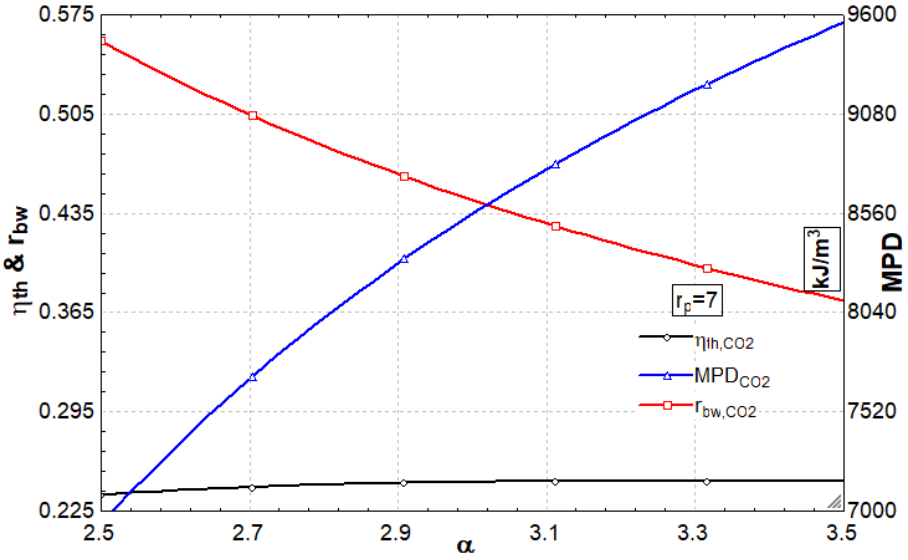

Figure 3. Effects of temperature ratio α on η_{th}, r_{bw} and *MPD*

It is seen that increasing the pressure ratio and temperature ratio increases the net work in the system if it is optimized by considering the temperature resistances of the turbine blades. Referring to figure 4, the pressure ratio is increased from 5 to 11 and also the temperature ratio increased from 2.5 to 3.5. While the temperature ratio is 2.5, the MPD is increased first by increasing the pressure ratio, and then decreased by a certain amount. Therefore, the pressure ratio should be optimized by taking into account the MPD. While the temperature ratios are 3 and 3.5, it is seen that the MPD increases by increasing the pressure ratio between 5 and 11. These increases seem to lead increases on w_{net} and *MPD*.

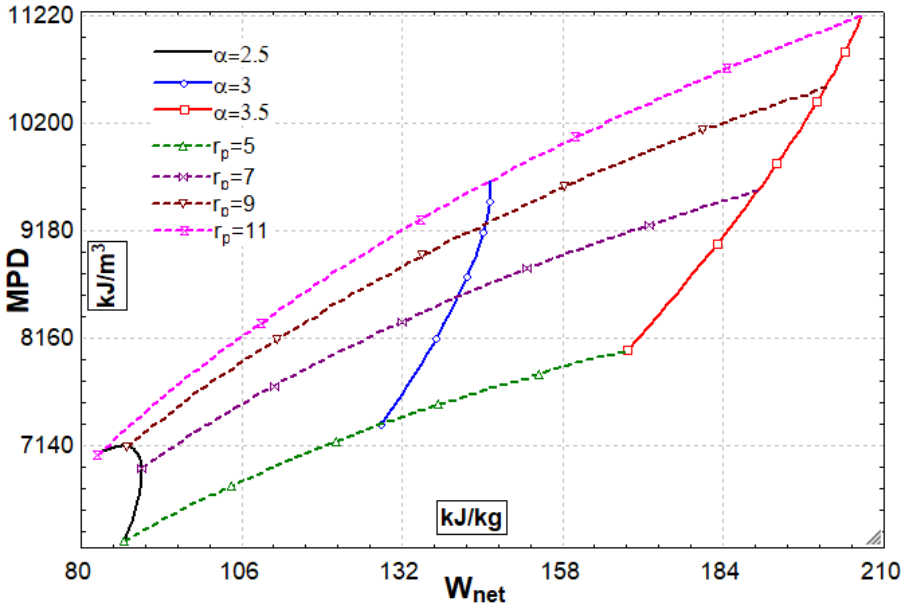

Figure 4. Variation of *MPD* and w_{net} with respect to various α and r_p

When optimizing the system, the pressure and temperature ratios need to be monitored in order to maximize the net work output and thermal efficiency. Figure 5 shows effect of increasing the temperature ratio and the pressure ratio on the thermal efficiency and *MPD*. An increase in thermal efficiency and an increase in *MPD* was observed with increasing temperature ratio. Similarly, thermal efficiency and *MPD* increase with increasing pressure ratio. The MPD reaches the highest value at the maximum pressure and maximum temperature ratios. The highest MPD will directly lead to lower machine dimensions which means low costs.

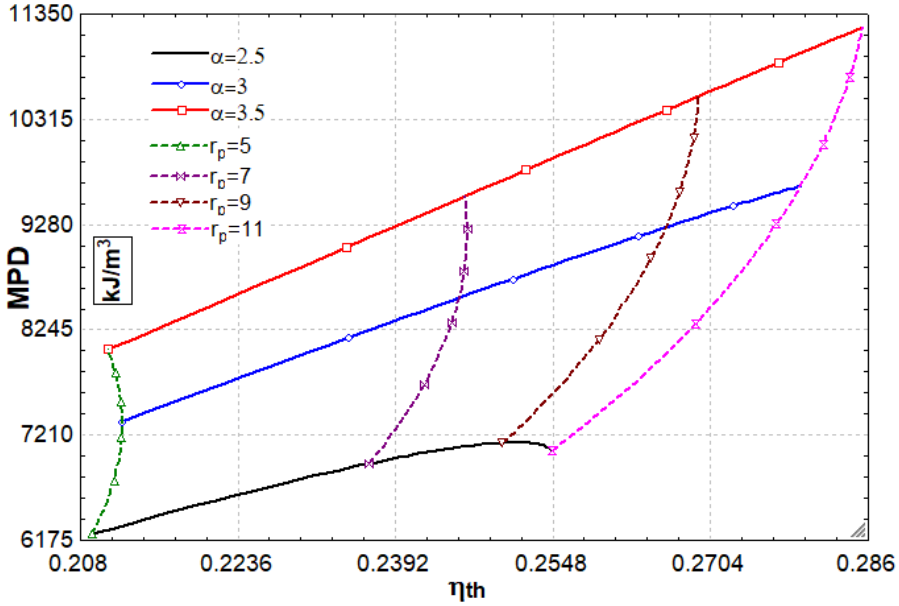

Figure 5. Variation of *MPD* and η_{th} with respect to various α and r_p

As it is known, the ratio of the work to the turbine work used to operate the compressor is called the back work. The increase in compressor work reduces the net work of the system. Thus, one can say; the less the back work, the higher the system efficiency. Figure 6 shows a decrease in the back work ratio with increasing the temperature ratio. However, an increase in *MPD* was observed with increasing temperature ratio from 2.5 to 3.5. Similarly, increasing the pressure ratio has led to an increase in the *MPD* and r_{bw}.

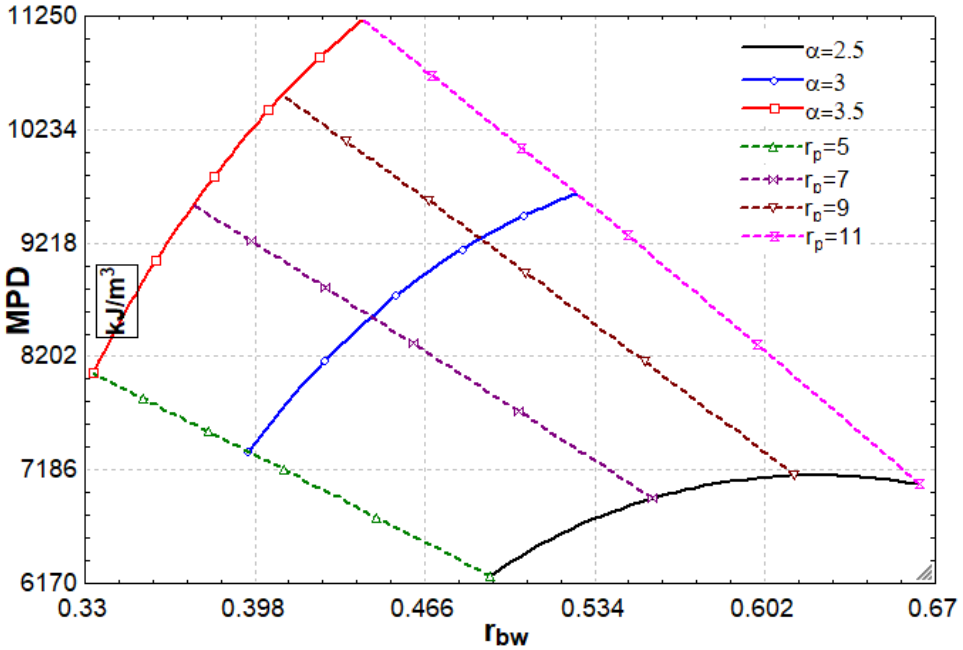

Figure 6. Variation of *MPD* and r_{bw} with respect to various α and r_p

When Figure 7 is examined, an increase in w_{net} is observed with increasing temperature ratio. As the temperature ratio increases, the thermal efficiency also increases at the same pressure ratio line which is an expected result. In addition, increasing the pressure ratio has also increased the thermal efficiency. When the figure is examined in detail, it is seen that the thermal efficiency increases with increasing pressure ratio for temperature ratio 2.5 and it increases with increasing pressure ratios at other temperature ratios but there is an optimum compression ratio that makes the net work maximum.

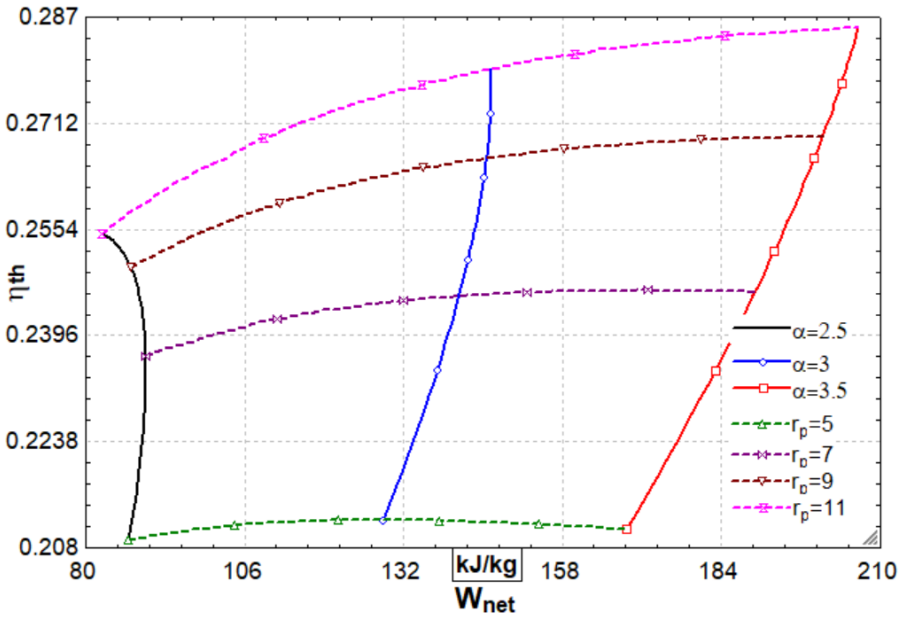

Figure 7. Variation of η_{th} and w_{net} respect to various α and r_p

CONCLUSION

The parameters which are obtained from analyzes were compared with those of a power performance criterion. And it is shown that design parameters at maximum power density give a chance to smaller cycle components and more efficient s-CO_2 Brayton power cycle. Major challenges of s-CO2 system can be expressed as, materials strength to improve reliability and cycle efficiency, identifying entire system design, developing oxy-combustors for direct fired system, model control strategies and lastly integration of fossil energy heat sources to the cycles. Due to loses in the cycle, the power and thermal efficiency are reduced by a certain amount, however, the maximum power density condition still gives a better performance than the maximum power output conditions. Effect of increasing the temperature ratio and the pressure ratio on the thermal efficiency and *MPD* have been examined. It can be concluded that *MPD* increases to a certain value with increasing r_p and then begins to decrease approximately when r_p is 9.286. An increase in thermal efficiency and an increase in *MPD* is observed with increasing α. Similarly, thermal efficiency and *MPD* increases with increasing pressure ratio. In addition, while r_p is 7 and constant, increasing α from 2.908 to 3.5 value, *MPD* increases 14.89%. To sum up, the results show that when system design optimizations are made, thermodynamic analyzes must also include *MPD* analysis in order to operate the system with smaller components.

NOMENCLATURE

cp	Specific heat capacity, kJ/kg.K
h	Specific enthalpy, kJ/kg
k	Isentropic coefficient
MPD	Maximum power density, kJ/m^3
TIT	Turbine inlet temperature, K
P	Pressure, kPa
q	Heat transfer, kJ/kg
r_p	Pressure ratio
r_{bw}	Back work ratio
T	Temperature, K

w	Specific work, kJ/kg

Greek Letters

η	Thermal Efficiency
α	Temperature Ratio

REFERENCES

[1] Sulzer G. Verfahren zur Erzeugung von Arbeit aus Warme. Swiss Pat 1950;269599.

[2] Feher E. Supercritical thermodynamic cycles for external and internal combustion engines. Astropower Inc Eng Rep May 1962 1962.

[3] Feher EG. The supercritical thermodynamic power cycle. Energy Convers 1968;8:85–90. https://doi.org/10.1016/0013-7480(68)90105-8.

[4] Cengel YA, Boles MA. Thermodynamics: An Engineering Approach. 4th edition. Boston: Mcgraw-Hill College; 2001.

[5] Dostal V. A Supercritical Carbon Dioxide Cycle for Next Generation Nuclear Reactors. Ph.D. Thesis. Massachusetts Institute of Technology, 2004.

[6] Parma EJ, Wright SA, Vernon ME, Rochau G, Suo-Anttila A, Al Rashdan A, et al. Supercritical CO2 Direct Cycle Gas Fast Reactor (SC-GFR) Concept. Proc. Supercrit. CO2 Power Cycle Symp. Boulder CO May, 2011, p. 24–25.

[7] Sienicki JJ, Krajtl L, Moisseytsev A. Utilization of the supercritical CO2 Brayton cycle with sodium-cooled fast reactors 2014.

[8] Persichilli M, Kacludis A, Zdankiewicz E, Held T. Supercritical CO2 power cycle developments and commercialization: why sCO2 can displace steam ste. Power-Gen India Cent Asia 2012.

[9] Escalona JMMD, others. The Potential of the Supercritical Carbon Dioxide Cycle in High Temperature Fuel Cell Hybrid Systems. Present. Therm. Power Group Univ. Seville Supercrit. CO2 Power Cycle Symp., 2011.

[10] Turchi CS, Ma Z, Dyreby J. Supercritical CO2 for application in concentrating solar power systems. SCCO2 Power Cycle Symp. RPI Troy NY, 2009, p. 1–5.

[11] Held TJ. Initial Test Results of a Megawatt-class Supercritical CO2 heat engine. 4th Int. Symp. Supercrit. CO2 Power Cycles Pittsburgh PA Sept, 2014, p. 9–10.

[12] Moore J, Brun K, Evans N, Bueno P, Kalra C. Development of a 1 MWe supercritical CO2 Brayton cycle test loop. Proc. 4 Th Int. Symp.-Supercrit. CO2 Power Cycles Pittsburgh Pa. Sept. 9, vol. 10, 2014.

[13] Cha J, Ahn Y, Lee J, Lee J, Choi H. Installation of the Supercritical CO2 Compressor Performance Test Loop as a First Phase of the SCIEL Facility. 4th Int. Symp. Supercrit. CO2 Power Cycles Pittsburgh PA Sept, 2014, p. 9–10.

[14] Wright SA, Conboy TM, Rochau GE. Break-even Power Transients for two Simple Recuperated S-CO2 Brayton Cycle Test Configurations. Sandia National Laboratories (SNL-NM), Albuquerque, NM (United States); 2011.

[15] Clementoni EM, Cox TL. Steady-state power operation of a supercritical carbon dioxide Brayton cycle. ASME Pap No GT2014-25336 2014.

[16] Sienicki J, Anton Moisseytsev, Dae Cho, Matthew Thomas, Rick Vilim, Yoichi Momozaki, et al. Recent Research & Development on the Supercritical Carbon Dioxide Brayton Cycle at Argonne National Laboratory - Supercritical CO2 Power Cycle Symposium 2009. http://www.sco2powercyclesymposium.org/resource_center/development_priorities/recent-research-development-on-the-supercritical-carbon-dioxide-brayton-cycle-at-argonne-national-laboratory (accessed July 5, 2017).

[17] Yan X. Dynamic analysis and control system design for an advanced nuclear gas turbine power plant. Massachusetts Institute of Technology, 1990.

[18] Moisseytsev A, Sienicki J. ANL Plant Dynamics Code and Control Strategy Development for the Supercritical Carbon Dioxide Brayton Cycle. 2009 Supercrit. CO2 Power Cycle Symp., 2009, p. 29–30.

[19] Casella F, Colonna P. Development of a Modelica dynamic model of solar supercritical CO2 Brayton cycle power plants for control studies. Proc. Supercrit. CO2 Power Cycle Symp., 2011, p. 1–7.

[20] Li Q, Flamant G, Yuan X, Neveu P, Luo L. Compact heat exchangers: A review and future applications for a new generation of high temperature solar receivers. Renew Sustain Energy Rev 2011;15:4855–4875.

[21] Dewson SJ, Thonon B. The development of high efficiency heat exchangers for helium gas cooled reactors. Int. Congr. Adv. Nucl. Power Plants ICAPP Pap., 2003.

[22] Haynes BS, Johnston A. High-effectiveness micro-exchanger performance. AIChE 2002 Spring Natl. Meet., 2002.

[23] Pecnik R, Colonna P. Accurate CFD Analysis of a Radial Compressor Operating with Supercritical CO2. Supercrit. CO2 Power Cycle Symp. Boulder Colo. USA, 2011.

[24] Bianchi N, Bolognani S, Luise F. Potentials and limits of high-speed PM motors. IEEE Trans Ind Appl 2004;40:1570–1578.

[25] Nagorny AS, Dravid NV, Jansen RH, Kenny BH. Design aspects of a high speed permanent magnet synchronous motor/generator for flywheel applications. Electr. Mach. Drives 2005 IEEE Int. Conf. On, IEEE; 2005, p. 635–641.
[26] Bianchi N, Bolognani S, Luise F. High speed drive using a slotless PM motor. IEEE Trans Power Electron 2006;21:1083–1090.
[27] Kolondzovski Z, Arkkio A, Larjola J, Sallinen P. Power limits of high-speed permanent-magnet electrical machines for compressor applications. IEEE Trans Energy Convers 2011;26:73–82.
[28] Gieras JF. Design of permanent magnet brushless motors for high speed applications. Electr. Mach. Syst. ICEMS 2014 17th Int. Conf. On, IEEE; 2014, p. 1–16.
[29] Mahaffey J, Kalra A, Anderson M, Sridharan K. Materials corrosion in high temperature supercritical carbon dioxide. 4th Int. Symp.-Supercrit. CO2 Power Cycles, 2014.
[30] Parks CJ. Corrosion of Candidate High Termperature Alloys in Supercritical Carbon Dioxide. Carleton University; 2013.
[31] De Barbadillo J, Baker BA, Gollihue R. Nickel-Base Superalloys for Advanced Power Systems–An Alloy Producer's Perspective. Proceeding 4th Symp. Heat Resist. Steels Alloys High Effic. USC Power Plants China, 2011.
[32] Sridharan K, Anderson M. Corrosion in supercritical carbon dioxide: materials, environmental purity, surface treatments, and flow issues. Battelle Energy Alliance, LLC; 2013.
[33] Wang P-Y, Hou S-S. Performance analysis and comparison of an Atkinson cycle coupled to variable temperature heat reservoirs under maximum power and maximum power density conditions. Energy Convers Manag 2005;46:2637–55. https://doi.org/10.1016/j.enconman.2004.11.005.
[34] Chen L, Lin J, Sun F, Wu C. Efficiency of an Atkinson engine at maximum power density. Energy Convers Manag 1998;39:337–41. https://doi.org/10.1016/S0196-8904(96)00195-1.
[35] Kodal A, Sahin B, Yilmaz T. A comparative performance analysis of irreversible Carnot heat engines under maximum power density and maximum power conditions. Energy Convers Manag 2000;41:235–48. https://doi.org/10.1016/S0196-8904(99)00107-7.
[36] Gonca G. Performance analysis and optimization of irreversible Dual–Atkinson cycle engine (DACE) with heat transfer effects under maximum power and maximum power density conditions. Appl Math Model 2016;40:6725–36. https://doi.org/10.1016/j.apm.2016.02.010.
[37] Sahin B, Kodal A, Yilmaz T, Yavuz H. Maximum power density analysis of an irreversible Joule-Brayton engine. J Phys Appl Phys 1996;29:1162.
[38] Gonca G, Sahin B, Ust Y, Parlak A. Comprehensive performance analyses and optimization of the irreversible thermodynamic cycle engines (TCE) under maximum power (MP) and maximum power density (MPD) conditions. Appl Therm Eng 2015;85:9–20. https://doi.org/10.1016/j.applthermaleng.2015.02.041.
[39] Chen L, Zheng J, Sun F, Wu C. Performance comparison of an endoreversible closed variable temperature heat reservoir Brayton cycle under maximum power density and maximum power conditions. Energy Convers Manag 2002;43:33–43. https://doi.org/10.1016/S0196-8904(01)00003-6.